

## Reprogramming Metabolism with Metformin Improves Tumor Oxygenation and Radiotherapy Response

Vanessa E. Zannella<sup>1,3</sup>, Alan Dal Pra<sup>1,2,4</sup>, Hala Muaddi<sup>1,5</sup>, Trevor D. McKee<sup>1</sup>, Shawn Stapleton<sup>1,6</sup>, Jenna Sykes<sup>1</sup>, Rachel Glicksman<sup>2,4</sup>, Selim Chaib<sup>1,8</sup>, Paul Zamir<sup>1,3</sup>, Michael Milosevic<sup>1,2,3,4</sup>, Bradly G. Wouters<sup>1,4,6,7,8</sup>, Robert G. Bristow<sup>1,2,3,4</sup>, and Marianne Koritzinsky<sup>1,3,4</sup>

### Abstract

**Purpose:** Tumor hypoxia is a negative prognostic factor in multiple cancers, due in part to its role in causing resistance to radiotherapy. Hypoxia arises in tumor regions distal to blood vessels as oxygen is consumed by more proximal tumor cells. Reducing the rate of oxygen consumption is therefore a potential strategy to reduce tumor hypoxia. We hypothesized that the anti-diabetic drug metformin, which reduces oxygen consumption through inhibition of mitochondrial complex I, would improve radiation response by increasing tumor oxygenation.

**Experimental Design:** Tumor hypoxia was measured in xenografts before and after metformin treatment using 2-nitroimidazole hypoxia markers quantified by immunohistochemistry (IHC), flow cytometry, and positron emission tomography (PET) imaging. Radiation response was determined by tumor growth delay and clonogenic survival in xenografts with and without administration of metformin. The impact of metformin use on outcome was assessed in 504 patients with localized prostate cancer treated with curative-intent, image-guided radiotherapy (IGRT) from 1996 to 2012. Three-year biochemical relapse-free rates were assessed using the Kaplan–Meier method.

**Results:** Metformin treatment significantly improved tumor oxygenation in two xenograft models as measured by IHC, flow cytometry, and PET imaging. Metformin also led to improved radiotherapy responses when mice were administered metformin immediately before irradiation. Clinically, metformin use was associated with an independent and significant decrease in early biochemical relapse rates ( $P = 0.0106$ ).

**Conclusion:** Our data demonstrate that metformin can improve tumor oxygenation and response to radiotherapy. Our study suggests that metformin may represent an effective and inexpensive means to improve radiotherapy outcome with an optimal therapeutic ratio. *Clin Cancer Res*; 19(24); 6741–50. ©2013 AACR.

### Introduction

The presence of tumor hypoxia is a negative prognostic factor in tumors treated with curative intent by radiotherapy

**Authors' Affiliations:** <sup>1</sup>Princess Margaret Cancer Centre and <sup>2</sup>Radiation Medicine Program, University Health Network; <sup>3</sup>Institute of Medical Science, <sup>4</sup>Department of Radiation Oncology, <sup>5</sup>Faculty of Medicine, <sup>6</sup>Department of Medical Biophysics, University of Toronto; <sup>7</sup>Selective Therapies Program, Ontario Institute for Cancer Research, Toronto, Ontario, Canada; and <sup>8</sup>Department of Radiation Oncology (Maastro Lab), GROW School for Oncology and Developmental Biology, Maastricht University, Maastricht, the Netherlands

**Note:** Supplementary data for this article are available at Clinical Cancer Research Online (<http://clincancerres.aacrjournals.org/>).

V.E. Zannella, A. Dal Pra, and H. Muaddi are the first authors and contributed equally to this work.

R.G. Bristow and Marianne Koritzinsky are the senior authors and contributed equally to this work.

**Corresponding Author:** Marianne Koritzinsky, 610 University Avenue, Rm 10-628, Toronto M5G 2M9, ON, Canada. Phone: 1-416-581-7841; Fax: 1-416-946-2984; E-mail: mkoritz@uhnresearch.ca

doi: 10.1158/1078-0432.CCR-13-1787

©2013 American Association for Cancer Research.

across multiple sites, including squamous cell carcinoma of the head and neck (1) and prostate carcinoma (2). Tumor cells located further than approximately 150µm from vessels experience "diffusion-limited" hypoxia as oxygen is consumed by the tumor cells more proximal to the vessels (3). Severely hypoxic yet viable cells are well documented to surround necrotic volumes (4), and these hypoxic cells are resistant to ionizing radiation (ref. 3). Several randomized clinical trials have shown the potential for improving radiotherapy efficacy by modifying the tumor microenvironment (5, 6). In these trials, attempts to increase tumor oxygenation before therapy were made using hyperbaric oxygen or an oxygen-rich gas like carbogen (95% O<sub>2</sub>, 5% CO<sub>2</sub>) in combination with systemic administration of vasodilating agents. In spite of positive results (5, 6), these strategies have not gained clinical traction due to practical limitations, toxicity, and relatively modest clinical benefit (7).

An alternative strategy to achieve improved tumor oxygenation is to decrease cellular oxygen consumption; a rational choice given that oxygen gradients arise from tumor cell respiration. Mathematical modeling suggests that

### Translational Relevance

In this study, we demonstrate that metformin can decrease tumor hypoxia and consequently increase radiation response. This provides a scientific rationale for combining metformin with radiotherapy in the clinic. Metformin is commonly prescribed as first line of treatment for patients with type II diabetes. It is generally well tolerated and already taken by numerous diabetic patients undergoing radiotherapy for cancer. Introduction of metformin to non-diabetic patients receiving radiation treatment is therefore of high feasibility, and could counteract tumor hypoxia that currently limits treatment efficacy. Identification of a novel mechanism by which metformin can improve radiation response will guide future biomarker evaluation and patient selection.

decreasing oxygen consumption could be significantly more efficient at improving tumor oxygenation than increasing oxygen supply (8). There is therefore ample rationale for combining pharmaceutical agents that decrease oxygen consumption with curative radiotherapy. This strategy has been explored *in vitro*, where a variety of respiration inhibitors have been shown to radiosensitize 3D spheroid models that contain viable hypoxic radioresistant cells in their interior (9–12). The respiration inhibitors meta-iodobenzylguanadine and arsenic trioxide have also been shown to increase radiation response in experimental tumor models (13, 14), but these agents are infrequently prescribed and may be associated with toxicities when combined with radiotherapy.

Metformin is a commonly prescribed biguanide used as a first-line treatment for type II diabetes. It efficiently and safely lowers blood glucose levels, and subsequently insulin, by inhibiting liver gluconeogenesis. Metformin's primary mechanism of action is considered to be direct inhibition of complex I activity in the mitochondrial electron transport chain (ETC; refs. 15–17). The ETC provides cellular ATP by transferring electrons from substrates provided by the citric acid cycle to molecular oxygen. Given that metformin is a well-tolerated drug already consumed by millions of patients with diabetes undergoing radiotherapy, we hypothesized that metformin's activity as a respiration inhibitor could lead to increases in tumor radiotherapy response through inhibition of tumor cell oxygen consumption and improved tumor oxygenation. This would constitute a novel mechanism in which tumor radioresponse is improved secondary to metabolic remodeling, rather than a change in the intrinsic radiosensitivity of the tumor cell.

### Materials and Methods

#### Cell lines and culture

LNCaP (CRL-1740) prostate carcinoma and HCT116 (CCL-247) colorectal carcinoma cells were from American

Type Culture Collection. The SCC-74B cell line was a generous gift from Dr. R. Grenman at Turku University Hospital (Finland), established from a squamous cell carcinoma of the tongue metastasized to a neck lymph node. The POP-092S cell line was created at Princess Margaret Cancer Center from a primary xenograft established from an adenocarcinoma of the sigmoid colon. LNCaP, HCT116, and SCC-74B cells were grown as adherent monolayers and kept in exponential growth phase. LNCaP and HCT116 cells were kept in RPMI and SCC-74B in MEM:F15, all supplemented with 10% FBS (all Gibco). POP-092S cells were grown in suspension in growth media to enrich for stem cells (18). Oxygen consumption was measured using a Seahorse XF96 Extracellular Flux Bioanalyzer (Seahorse Bioscience).

#### Irradiation and clonogenic survival

Cells were irradiated using a  $^{137}\text{Cs}$  Nordion Gammacell unit at a dose rate of 1.03 Gy/min. Metformin was present for 30 minutes before, and 1 hour after, irradiation. Cells were then trypsinized and single cells plated for clonogenic survival at low density in triplicate. After 14 days, colonies were fixed, stained (0.2% methylene blue in 80% ethanol), and counted if containing more than 50 cells. Surviving fraction was calculated as the number of colonies divided by the number of seeded cells in the treated population, corrected by the same ratio for the untreated.

#### Xenograft establishment and growth

All animal experiments were performed under protocols approved by the Ontario Cancer Institute's Animal Care Committee, according to the regulations of the Canadian Council on Animal Care. HCT116 and POP-092S donor tumors were grown in the right biceps femoris muscle and under the left renal capsule, respectively. Tumor fragments measuring 2.0 mm were implanted subcutaneously into the right flank of syngeneic mice. Severe combined immunodeficient mice were used for all experiments except tumor growth delay after irradiation, where we used non-radio-sensitive athymic CD-1 nude mice. Tumor growth was monitored by caliper measurements 3 times a week. All surgical procedures and tumor imaging were carried out under anesthesia (3% isoflurane induction, 1% maintenance). For measurements of oxygen consumption rates (OCR), tumor-bearing mice were sacrificed and 23 tumor fragments weighing 7–10 mg were immediately placed in individual wells in the Seahorse XF96 Extracellular Flux Bioanalyzer (Seahorse Bioscience).

#### Quantification of tumor hypoxia

Mice carrying 200 mm<sup>3</sup> HCT116 tumors or 1,000 mm<sup>3</sup> POP-092S tumors were injected intraperitoneally with 120 mg/kg pimonidazole (Hydroxyprobe-1, Chemicon International). After 2 hours, mice started breathing carbogen (95%O<sub>2</sub>, 5%CO<sub>2</sub>) or received 100 mg/kg metformin *i.v.* After 10 minutes, 10 mg/kg EF5 (2-(2-Nitro-1H-imidazole-1-yl)-N-(2,2,3,3,3-pentafluoropropyl)acetamide), a kind gift from Dr. C. Koch (University of Pennsylvania,

Philadelphia, PA) was injected intraperitoneally. Three hours later, 50 mg/kg Hoechst 33342 (Invitrogen) was injected intravenously and mice sacrificed by cervical dislocation. One tumor half was immediately frozen in liquid nitrogen, the other half was processed for flow cytometry.

### Immunohistochemistry

Tumor sections measuring 5  $\mu$ m were fixed with 2% paraformaldehyde and scanned for Hoechst autofluorescence using an Olympus Fluorescence upright Microscope with Metamorph software. They were stained with FITC/Cy3/Cy5-conjugated antibodies recognizing pimonidazole (Hydroxyprobe, Chemicon International), EF5 (Dr. C. Koch, University of Pennsylvania), and CD31 (BD Pharmingen), respectively, and DAPI (Sigma) for DNA. Scans were aligned with ImagePro and analyzed with Definiens TissueStudio suite, including only viable tumor tissue (Supplementary Fig. S1A). A threshold for background was applied to each individual stain signal and subsequently either the average intensity or a binarized fractional positive area (Supplementary Fig. S1B) was calculated.

### Flow cytometry

Tumors were disaggregated using DNase I, *Streptomyces griseus* protease, and collagenase IX, filtered, fixed, and permeabilized using formaldehyde and Triton X-100 (all Sigma). Cells were blocked with 10% skim milk, 1.5% lipid-free albumin, 5% mouse serum and stained with FITC-anti-pimonidazole, Cy5-conjugated antibody against EF5, and DAPI. Flow cytometry was performed on a BD Biosciences LSR II and analyzed with FlowJo (Tree Star Inc.). Only the POP-092S tumors yielded sufficient cell numbers for analysis.

### <sup>18</sup>F-FAZA-PET imaging and analysis

Hypoxia was assessed using micro-PET imaging of the hypoxia tracer <sup>18</sup>F-FAZA (fluoroazomycin-arabinofuranoside). Mice were administered 100 mg/kg metformin intravenously, and 30 minutes later injected with approximately 11 MBq of <sup>18</sup>F-FAZA i.v. (Centre for Probe Development and Commercialization). After 140 minutes, the mice were anesthetized using isoflurane, scanned for 20 minutes with the Focus 220 micro-PET (Siemens Preclinical Solutions), and computed tomography (80 kV, 70 mA, eXplore Ultra, GE Healthcare). Image registration and contouring was performed using Inveon Research Workplace (Siemens). Tumor and muscle tissues were contoured and the %injected dose/gram was exported for each voxel of each tissue and further analyzed in MatLab (Mathworks). A normal distribution was fit to the %ID/g muscle histogram, defining well-oxygenated tissue. The distribution of tumor voxels was then fit to a function defined as the sum of two normal distributions; the first distribution representing well-oxygenated tissue derived from muscle and the second distribution representing the hypoxic voxels. The hypoxic tumor fraction was defined as the fractional area under the curve of the hypoxic distribution.

### Xenograft irradiation and growth delay

Mice bearing 200 mm<sup>3</sup> HCT116 tumors were injected intravenously with 100 mg/kg metformin or saline 30 minutes before irradiation. Anesthetized mice underwent a cone-beam CT scan followed by image-guided tumor radiation at 2.92 Gy/min using two beams from XRAD 225. Mice affected by gastrointestinal toxicity (less than 5%) were excluded from the study. Tumor growth was monitored 3 times a week by caliper measurements.

### Ex vivo clonogenic assays

Mice bearing 200 mm<sup>3</sup> HCT116 tumors, established by subcutaneous injection of  $2 \times 10^6$  cells, were irradiated without anesthesia using a Gammacell. To create completely hypoxic tumors, one group of mice was sacrificed 5 minutes before irradiation, while the other group was sacrificed immediately following irradiation. Tumors were excised, dissociated, and colony-forming assays were performed, correcting for viability using Trypan blue exclusion.

### Patient cohort and treatment characteristics

This study was approved by the UHN Research Ethics Board (REB# 12-5365-CE). A detailed retrospective chart review was performed of 504 patients treated with curative external beam radiotherapy for clinical stage T1-T4, N0-X, M0 adenocarcinoma of the prostate cancer at Princess Margaret Hospital between 1996 and 2012. The clinical data are summarized in Supplementary Table S1, including the use of metformin or other oral hypoglycemic drugs (e.g., sulfonylureas, thiazolidinediones, meglitinide) and/or insulin. The total radiotherapy dose was escalated over the period of accrual in a series of separate phase I/II studies as previously published (19). The median radiation dose for the entire cohort was equivalent to 78 Gy in 2 Gy fractions. Patients were followed at 6 monthly intervals after completing treatment with clinical examination and prostate specific antigen (PSA).

### Statistical analysis

For studies *in vitro* or in experimental tumor models, two-sided *t* tests or log-rank tests were used to assess statistical significance. For clinical data, the primary outcome was biochemical relapse-free rate (bRFR) following the start of radiotherapy. Biochemical relapse was defined by the Phoenix criteria as a posttreatment PSA nadir plus 2 ng/mL or treatment of salvage hormones due to a rising PSA as previously described (19). Patients who did not experience a biochemical relapse by their last known PSA date were considered censored. A Cox proportional-hazards model was used to determine whether metformin use influenced biochemical failure after radiotherapy independent of standard clinical prognostic factors. The proportional hazards assumption was checked for each variable by looking at the Schoenfeld residuals. As the proportional hazards assumption was found to be violated for metformin use, a Cox regression model was used to model metformin as a time-varying coefficient, adjusting for clinical T-category (T1 vs. T2+), Gleason score (6 vs. 7 vs. 8+), pretreatment

PSA (continuous), and the use of hormonal treatment (Y vs. N) as previously described (2). All analyses were done using SAS version 9.2 and R version 2.12.1. A two-sided  $P$  of 0.05 was used to assess statistical significance.

As a complimentary analysis, patients with and without record of metformin use were propensity score matched according to a list of important clinicopathologic covariates. The logit of the propensity score was calculated by forming a logistic regression model for metformin use with all the main effects and all two-way interactions of the following variables: Gleason score (6 vs. 7 vs. 8–9), pre-treatment PSA (continuous), age at the start of treatment (continuous), follow-up time (years, continuous), biologic equivalent dose (BED, continuous), hormone therapy (yes vs. no), and T-category (T1 vs. >T2). The best model was chosen using backwards selection. A one-to-one greedy matching algorithm was performed using a width of 0.2 of the SD of the logit of the propensity score (SAS macro

gmatch available at Mayo Clinic website; ref. 20). Missing values of covariates were excluded. Covariate balance of the resulting cohort was assessed by ensuring all standardized differences were less than 10 (21).

## Results

We measured oxygen consumption ratios (OCRs) *in vitro* in the presence and absence of metformin in prostate carcinoma (LNCaP), head and neck squamous cell carcinoma (SCC-74B), and colorectal adenocarcinoma (HCT116 and POP-092S) cells. Metformin caused a significant dose- and time-dependent decrease in oxygen consumption in all cell lines (Fig. 1A). Substantial differences were observed across the lines in terms of both metformin sensitivity and response kinetics (Fig. 1B). The most metformin-sensitive line was the prostate cell line LNCaP, which demonstrated a significant ( $P < 0.05$ ) reduction in respiration at an *in vitro* concentration of metformin

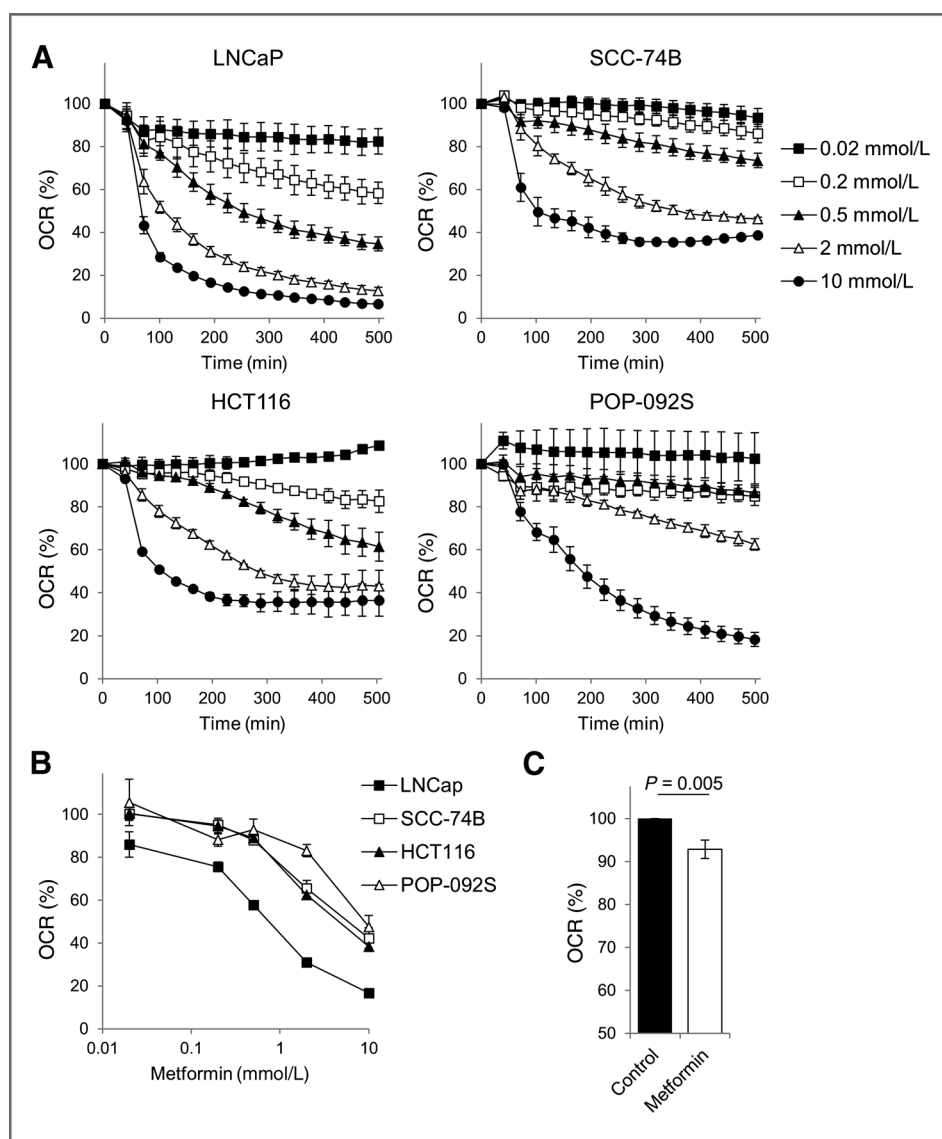


**Figure 1.** Metformin inhibits oxygen consumption. A, the OCR of LNCaP, SCC-74B, HCT116, or POP-092S cells were measured over time after injection of various concentrations of metformin using the Seahorse Bioanalyzer. Data are normalized to basal OCR before metformin injection and represent 3 independent experiments  $\pm$  SEM. B, relative OCR compared across the 4 cell lines at 3 hours post-metformin injection. LNCaP was more sensitive than other cell lines, which was statistically significant ( $P < 0.05$ ) for doses  $>0.2$  mmol/L metformin. C, HCT116 xenografts were excised 30 minutes after intravenous administration of 100 mg/kg metformin to the tumor-bearing mice. OCR were measured on 23 pieces from each tumor, weighing 7–10mg. Data show average OCR  $\pm$  SEM,  $n = 7$ .

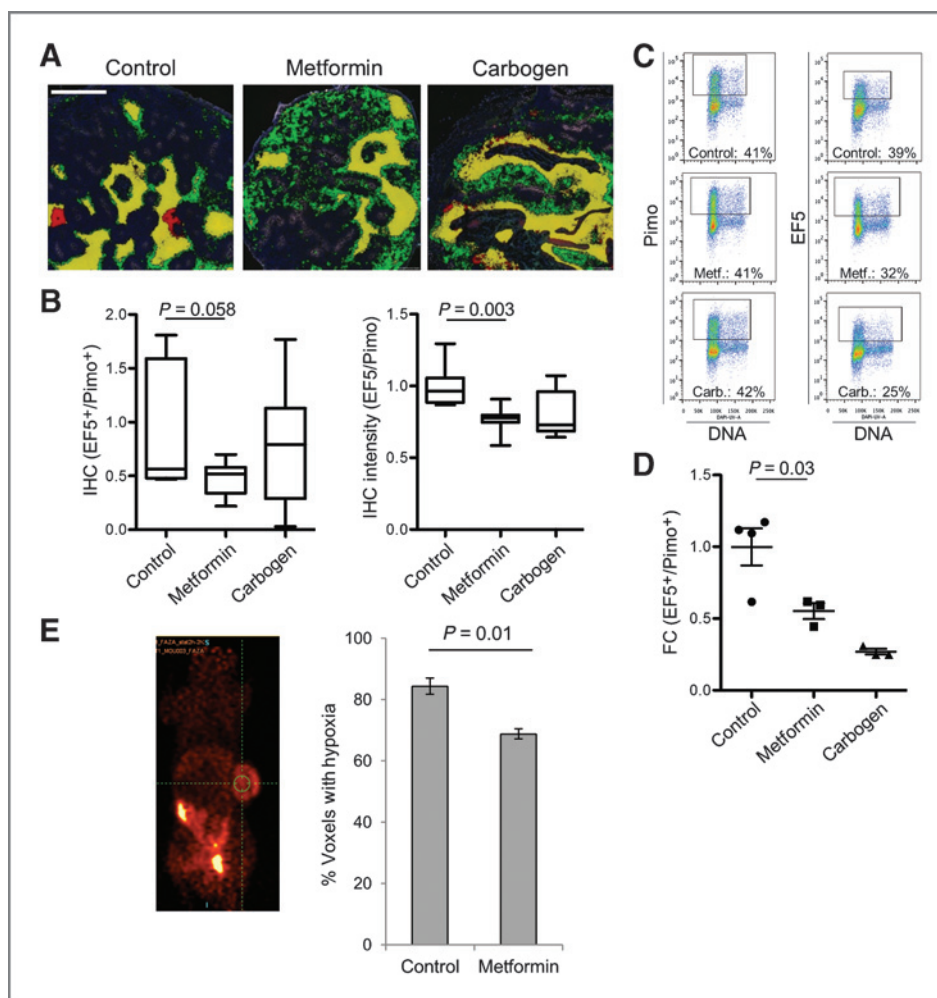
typically achieved in the plasma of patients diabetes (0.02 mmol/L; Fig. 1A and B). To determine whether metformin could also inhibit oxygen consumption *in vivo*, we injected mice bearing HCT116 xenografts with 100 mg/kg metformin and measured OCRs in multiple tumor pieces *ex vivo*. This acutely administered dose corresponds to 25% of the daily oral dose taken by patients with diabetes (22). Metformin-treated tumors demonstrated reduced rates of oxygen consumption compared with controls (Fig. 1C, 7% reduction;  $P = 0.005$ ). These data show that metformin can reduce oxygen consumption *in vitro* and *in vivo* at clinically relevant doses.

As tumor hypoxia arises in large part from oxygen consumption, we determined whether metformin could improve oxygen distribution in tumors. To this end, we first injected tumor-bearing mice with the 2-nitroimidazole pimonidazole (pimo) which binds and labels hypoxic cells in the absence of oxygen. After pimo had cleared the bloodstream (2 hours), we injected 100 mg/kg metformin or administered carbogen, followed by injection of a second 2-nitroimidazole, EF5, along with a perfusion marker, Hoechst. This strategy allows for detection of hypoxic tumor cells before and after the intervention, using antibodies

specific for pimo and EF5. Using quantitative immunohistochemistry (IHC; Supplementary Fig. S1A), we found that metformin substantially reduced hypoxia in HCT116 tumors. Figure 2A shows examples of tumor sections where hypoxic cells before treatment (pimo+) are pseudo-colored green, and hypoxic cells following treatment (EF5+) are pseudo-colored red. In untreated tumors, most cells appear yellow as there are minimal changes in oxygenation in the time period between administrations of the two hypoxic cell markers (Fig. 2A). A few cells stain for only one marker, consistent with transient hypoxia due to changes in red blood cell flux. In tumors from mice treated with metformin or carbogen, there was a significant decrease in EF5 (red) relative to pimo (green), reflecting tumor reoxygenation. Both the relative fraction of EF5 to pimo-positive cells, as well as the EF5 to pimo intensity ratio (Fig. 2B) dropped upon treatment with metformin. Similar results were observed in the POP-092S colon xenograft model (Supplementary Fig. S1C and S1D). There were no consistent changes in tumor perfusion upon metformin treatment as measured by Hoechst staining (data not shown).

IHC allows spatial analysis of the tumor microenvironment with single-cell resolution, but represents only a

**Figure 2.** Metformin increases tumor oxygenation. **A:** Mice bearing HCT116 xenografts were administered the hypoxic cell marker pimonidazole (pimo) 2 hours before intravenous injection of 100 mg/kg metformin or carbogen breathing (95% O<sub>2</sub>, 5% CO<sub>2</sub>), followed by administration of a second hypoxic cell marker, EF5. After 3 hours, tumors were excised, sections stained and signals binned. Green: Pimo+, Red: EF5+, Yellow: Pimo+EF5+. Examples from each group are shown. Scale bar represents 500  $\mu$ m. **B:** Quantification of tumor hypoxia across all HCT116 tumors from IHC. Left: the ratio of EF5+/Pimo+ from binned images. Right, the intensity ratio of EF5/Pimo from non-binned images ( $n = 4-5$ ). **C:** Mice bearing POP-092S tumors were treated as in (A). After tumor excision, cells were dissociated and fraction of pimo+ and EF5+ cells quantified by flow cytometry. Examples from each group are shown. **D:** Quantification of tumor hypoxia across all POP-092S tumors from flow cytometry. The ratio of EF5+/Pimo+ is shown for each separate tumor. **E:** Groups of mice carrying HCT116 tumors were injected with <sup>18</sup>F-AZA after 100 mg/kg metformin and imaged with  $\mu$ PET. An example image is shown on the left. Right, the average fold change in hypoxic tumor fraction  $\pm$  SEM ( $n = 3$ ).



subregion of the tumor. To probe the tumor microenvironment on a scale representative of the whole tumor, we dissociated POP-092S tumors and measured hypoxia before and after metformin treatment using flow cytometry. Similar to IHC results, the fraction of hypoxic (EF5+) cells dropped significantly following metformin treatment, reflecting widespread tumor reoxygenation (Fig. 2C and D). The same approach was undertaken for LNCaP xenografts. These tumors supported very low levels of hypoxia, allowing quantitative analysis of only 4. Among these, metformin resulted in a substantial drop in hypoxia following metformin treatment (Supplementary Fig. S1E). This robust response is consistent with the superior sensitivity of LNCaP cells to metformin (Fig. 1B), but firm conclusions cannot be drawn in light of the low numbers. Finally, in SCC-74B xenografts we experienced a much increased inter-tumor variability compared with the other models, and no evidence of metformin-induced altered oxygenation (data not shown). Hence, 3 of 4 tumor models

provided data supporting a substantially reduced hypoxic fraction following metformin treatment.

Since noninvasive hypoxia imaging is entering clinical practice, we assessed whether this modality could also resolve metformin-induced changes in tumor oxygenation. Groups of mice bearing HCT116 tumors were injected with the positron-emitting 2-nitroimidazole  $^{18}\text{F}$ -FAZA and the percentage of tumor voxels containing hypoxia was estimated from micro-PET imaging. Consistent with results obtained using antibody-based IHC and flow cytometry,  $^{18}\text{F}$ -FAZA-PET analysis demonstrated a significant ( $P = 0.01$ ) reduction in the hypoxic tumor volume after metformin treatment (Fig. 2E). Taken together, results presented in Fig. 2 demonstrate that metformin improves oxygenation as assessed at both micro- and macroscopic levels.

To test whether the reduction in tumor hypoxia in metformin-treated animals was sufficient to improve radiotherapy response, we irradiated HCT116 xenografts with a subcurative, single dose of 15 Gy and measured the time

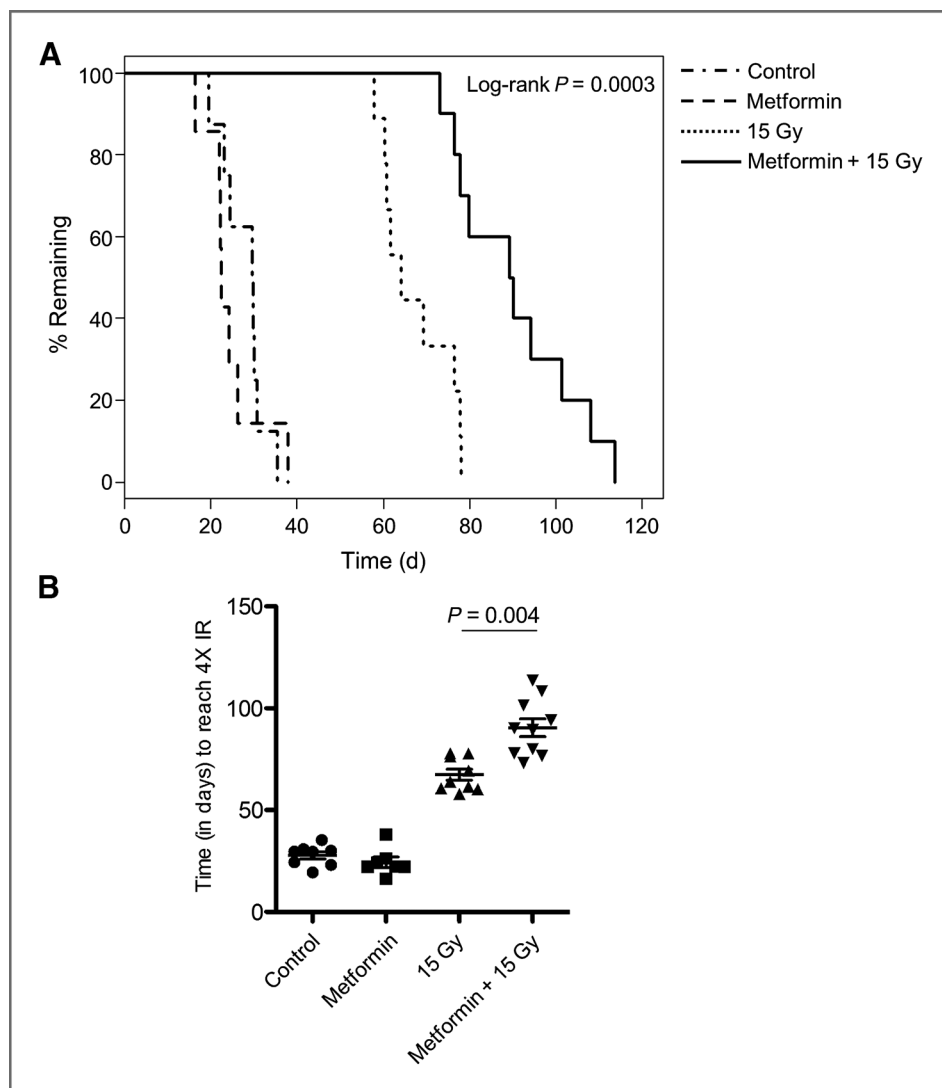


**Figure 3.** Mice bearing HCT116 xenografts were injected with saline or 100 mg/kg metformin 30 minutes before irradiation with 15 Gy. Tumor growth was monitored over time and endpoint was defined as  $4\times$  the irradiated tumor volume. A, Kaplan-Meier representation of the data. B, Individual tumors' time to reach  $4\times$  irradiated volume.

required for tumors to reach 4 times the irradiated volume. As expected, a single dose of metformin alone did not alter tumor growth (Fig. 3A and B). However, metformin administered 30 minutes before irradiation significantly increased tumor growth delay (log-rank  $P = 0.0003$  in A and  $t$  test  $P = 0.004$  in B). This increase in tumor response was not due to a change in cellular intrinsic radiosensitivity of oxygenated cells, as metformin treatment *in vitro* did not influence response (Supplementary Fig. S2A). To corroborate this conclusion, we assessed the colony-forming ability of tumor cells *in vitro* following irradiation *in vivo*. We irradiated half of the tumor-bearing mice immediately following cervical dislocation, which renders all tumor cells hypoxic regardless of OCRs. Consistent with the proposed mechanism, we observed that metformin only potentiated radiation-induced cell death in tumors from live, air-breathing mice (Supplementary Fig. S2B). These results strongly suggest that metformin increases tumor radiation response *in vivo* by reducing the hypoxic tumor fraction.

We reasoned that if metformin causes increased tumor oxygenation and radiation response, patients with diabetes taking metformin might have better outcomes following curative radiotherapy. We had previously shown that the presence of intraglandular hypoxia leads to early biochemical failure (based on biochemical relapse-free rate; bRFR) following radiotherapy for localized prostate cancer (2). We therefore determined whether metformin altered early biochemical failure in 504 men undergoing similar curative prostate cancer radiotherapy that had differential metformin use (see cohort characteristics in Supplementary Table S1), with a median follow up from start of radiotherapy of 81.6 months (range 2.4–153.6). Within this cohort, we identified 114 patients taking metformin at the time of radiotherapy. On univariate analysis, the effect of metformin on bRFR was maximal early in follow-up [HR = 0.32; 95% confidence interval (CI): 0.11–0.92;  $P = 0.034$ ] and diminished with increasing time ( $P = 0.019$ ). Within a

**Table 1.** Multivariate predictive models for bRFR after prostate cancer radiotherapy

Variable	HR (95% CI)	P
Metformin (Y vs. N) <sup>a</sup>	0.228 (0.073–0.709)	0.0106
Metformin with time <sup>b</sup>	1.018 (1.004–1.033)	0.0138
Systemic Treatment		
ADT (Y vs. N)	0.729 (0.516–1.030)	0.0734
Clinical Prognostic Factors		
Gleason (7 vs. 6) <sup>c</sup>	1.044 (0.705–1.547)	0.8296
Gleason (8-9 vs. 6) <sup>c</sup>	2.234 (1.159–4.306)	0.0163
PSA (Continuous)	1.027 (1.013–1.033)	0.0002
T-stage (T2+ vs T1) <sup>c</sup>	1.390 (0.992–1.948)	0.0555

<sup>a</sup>Effect of metformin on bRFR.

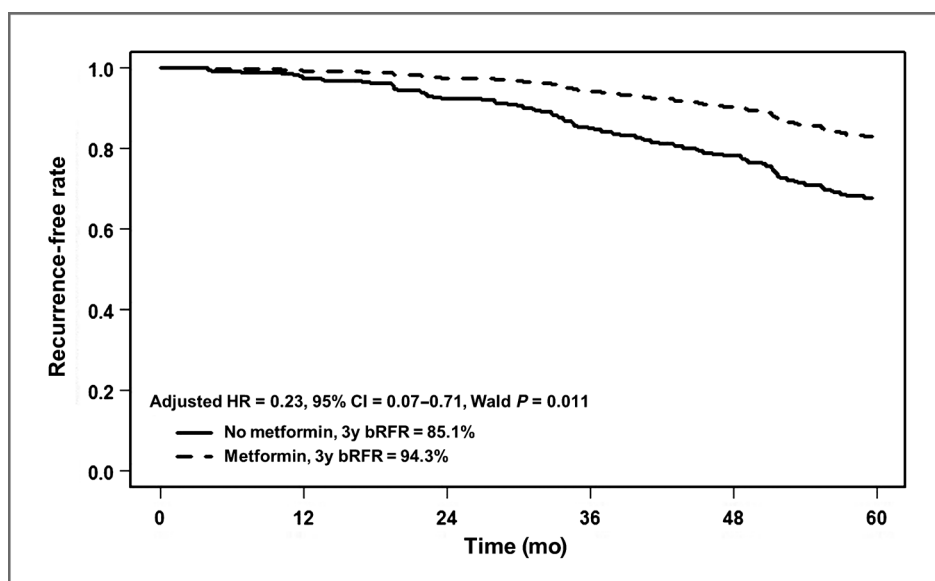
<sup>b</sup>Time-dependent effect of metformin.

<sup>c</sup>Used as reference variable.

Abbreviations: ADT, androgen deprivation therapy; bRFR, biochemical relapse-free rate.

multivariate model, metformin use and a metformin interaction-with-time term, were both used to determine an independent effect of metformin on bRFR (see Table 1 and Fig. 4). Consistent with the preclinical data, the use of metformin was a significant and independent factor reducing early biochemical relapse after radiotherapy (after correcting for clinical covariates). As a complementary statistical approach, we also assessed the independent prognostic role of metformin using a propensity-score, matched analysis of 172 patients (Supplementary Fig. S3) in which 86 patients taking metformin were matched on the basis of previously reported covariates to patients in a control group (yielding proper balance among all covariates). In this subanalysis, the bRFR at 3 years for patients on metformin was 92% as compared to 81% in the control group

**Figure 4.** This plot shows biochemical recurrence-free rates over time in a cohort of 504 prostate cancer patients, adjusting for known clinical factors including PSA, T category, Gleason score and androgen deprivation therapy use.



(adjusted HR = 0.63; 95% CI: 0.32–1.24;  $P = 0.06$ , stratified log-rank; see Supplementary Fig. S4). A cumulative incidence analysis considering deaths without prior biochemical recurrence to be competing risks (data not shown) confirmed these findings.

Taken together, our data suggest that metformin can provide a benefit to patients with cancer treated with radiotherapy through its effects on reprogramming tumor metabolism and increasing tumor oxygenation.

## Discussion

Epidemiologic and retrospective studies have suggested that metformin may act as a cancer prevention and/or therapeutic agent (23). Two different mechanisms of anticancer activity have been proposed for metformin and other biguanides. The first is due to their ability to reduce circulating insulin levels, removing a potential growth-stimulating factor in cancer cells expressing the insulin receptor (23, 24). The second is through direct effects on metabolic activity of cancer cells, resulting in activation AMPK and subsequent inhibition of mTOR activity (23–26). Here, we propose a new mechanism for metformin with specific application to cancers treated with radiotherapy—the inhibition of oxygen consumption (16,17), with consequential reoxygenation of radio-resistant hypoxic cells; this effect is independent of an effect on tumor cell radiosensitivity.

In addition to tumor hypoxia, intrinsic cellular radiation resistance and high proliferation rates limit the efficacy of radiotherapy. In the preclinical tumor model used here, we found no evidence that metformin affects intrinsic radiosensitivity. Some studies have reported that metformin can function as a cellular radiosensitizer (27–29), but this is clearly cell line dependent (30, 31). Furthermore, it is uncertain whether metformin associated changes in radiosensitivity would offer any therapeutic ratio benefit, as the response of normal tissues to combined radiotherapy-metformin is currently unknown. Reports have suggested that in cell lines in which metformin increases radiosensitivity, continuous administration of metformin before and after radiation can increase tumor growth delay (26, 28, 30). In these studies, it is difficult to attribute the effects of metformin to specific mechanism(s), as they may include alterations of radiosensitivity and tumor cell proliferation. Metformin alone also affects tumor growth in this setting, rendering the possible additive versus synergistic effect with radiation unclear. Our xenograft study was designed to provide proof-of-principle that metformin improves radiation response specifically by the mechanism of increased tumor oxygenation *in vivo*. This was achieved by selecting a cell line that was not radiosensitized by metformin *in vitro* or *in vivo* (Supplementary Fig. S2), and by delivering a single dose of metformin before radiation that alone had no effects on xenograft growth. Metformin treatment did also not alter blood glucose levels in the experimental animals (Supplementary Fig. S5).

According to standard and U.S. Food and Drug Administration-recommended guidelines on dose-conversion

between species (22), the single intravenous dose of 100 mg/kg metformin in mice, that was used in all *in vivo* experiments here, corresponds to about 25% of the daily dose taken orally by patients with diabetes (2,000 mg). Metformin is known to accumulate in some tissues, rendering the concentrations substantially higher than the steady-state plasma level (32). Tissue accumulation is likely dependent on expression of plasma membrane organic cation transporters (OCT) and multidrug and toxin extrusion (MATE) proteins (15). Ultimately, the efficacy of metformin to inhibit oxygen consumption will rely on the local concentration at the mitochondria, which may depend on other additional factors. These considerations combined with our data demonstrating 7% reduction in OCRs in tumors upon metformin administration (Fig. 1C) strongly suggest that clinically relevant metformin doses can modify tumor respiration. Mathematical modeling by Secomb and colleagues indicates that this magnitude of reduced oxygen consumption could have substantial impact on the hypoxic tumor fraction (8), in line with our measurements (Fig. 2).

Taken together, our results indicate that metformin can substantially reduce the fraction of viable hypoxic cells that currently limit the efficacy of radiation treatment. This observation provides a novel mechanism and scientific rationale for combining metformin with radiotherapy in the clinic. The knowledge of metformin's specific mechanism of action provided here has profound implications for translating these findings into future clinical application. Metformin may be particularly useful in the context of altered fractionation radiotherapy schedules such as hypofractionation (doses more than 2 Gy per fraction). According to results from mathematical modeling of tumor responses to radiotherapy, hypofractionation can result in a significant decrease in tumor cell killing compared with standard fractionation as a result of tumor hypoxia (33). Hypoxia modifying agents have therefore been suggested to be particularly important during hypofractionated radiotherapy schedules (7, 34). Metformin may thus have a specific role in prostate cancer, where hypofractionated radiotherapy schemes are increasingly used.

We observed that patients with prostate cancer taking metformin had decreased early biochemical failure after radiotherapy. Although this effect cannot be directly attributed to reduced tumor hypoxia, it is consistent with the expected impact that an increase in tumor oxygenation would have. It is enticing that metformin improves rates of early biochemical relapse with very similar effect size and interaction with time as oxygen status itself in a similar patient cohort (2). Importantly, early biochemical failure after radiotherapy (e.g., within 18 months) has been observed to be a surrogate of prostate cancer-specific lethality (35) and if metformin use specifically reduced this risk, it could lower prostate cancer-specific mortality. Indeed, a recent retrospective study observed lower rates of biochemical relapse, distant metastasis, prostate cancer-specific mortality and overall mortality after combined radiotherapy-metformin use (27). In a large population-based

retrospective study, Margel and colleagues have shown that for every additional 6 months of metformin treatment, there is a 24% decrease of prostate cancer-specific mortality and a decrease in all-cause mortality that declines over time, independent of treatment modality. Despite a lack of important details of the treatment, a subgroup analysis of 937 patients (24.4% of the entire cohort) who received radiotherapy as primary treatment showed a 48% decrease in prostate cancer-specific mortality (adjusted HR, 0.56; 95% CI: 0.3–0.85;  $P = 0.09$ ; ref. 36). Other results from a smaller cohort of patients with head and neck cancer treated with postoperative radiotherapy or patients with esophageal cancer treated with neoadjuvant chemoradiation showed that metformin use leads to lower locoregional relapse rates and improved complete pathologic response (30, 37). These data are all consistent with metformin enhancing radiotherapy response *in vivo*.

The findings presented here from mechanistic studies in experimental tumor models and subsequent supportive clinical data, indicate that changes in tumor oxygenation contribute to the scientific rationale for pursuing metformin (and similar-acting agents) as a novel radiotherapy-enhancing drug. Novel strategies to overcome the barrier of tumor hypoxia in radiation treatments with curative intent are needed, and metformin may represent a safe and efficacious approach. Application of this strategy should incorporate use of biomarkers to help identify those patients most likely to benefit of the combination. Pretreatment tumor hypoxia by gene signatures or extrinsic markers such as pimonidazole (IHC) or FAZA (PET) represent potentially important biomarkers for patient stratification. Furthermore, assessment of perfusion-limited versus diffusion-limited hypoxia may be important as metformin is only expected to affect diffusion-limited hypoxia. In fact, the large inter-tumor heterogeneity in (EF5+/Pimo+) observed in SCC-74B (data not shown) suggests that tumor hypoxia arises predominantly from the lack of perfusion in this model and could explain the lack of response *in vivo*. Other genetic tumor characteristics including the expression of OCT/MATE transporters represent additional potential biomarkers of response. Evaluation of biomarkers and patient stratification will be key to applying metformin as a means to modify

the tumor microenvironment in combination with radiotherapy for future personalized cancer medicine.

#### Disclosure of Potential Conflicts of Interest

B.G. Wouters is employed as a professor (other than primary affiliation; e.g., consulting) at Maastricht University and has a commercial research grant from Pfizer. No potential conflicts of interest were disclosed.

#### Authors' Contributions

**Conception and design:** V.E. Zannella, A. Dal Pra, M. Milosevic, B.G. Wouters, R.G. Bristow, M. Koritzinsky

**Development of methodology:** V.E. Zannella, A. Dal Pra, H. Muaddi, T.D. McKee, B.G. Wouters, R.G. Bristow, M. Koritzinsky

**Acquisition of data (provided animals, acquired and managed patients, provided facilities, etc.):** A. Dal Pra, H. Muaddi, T.D. McKee, S. Chaib, R. Glicksman, P. Zamiara, M. Milosevic, B.G. Wouters, R.G. Bristow, M. Koritzinsky

**Analysis and interpretation of data (e.g., statistical analysis, biostatistics, computational analysis):** V. Zannella, A. Dal Pra, H. Muaddi, T.D. McKee, S. Stapleton, J. Sykes, M. Milosevic, B.G. Wouters, R.G. Bristow, M. Koritzinsky

**Writing, review, and/or revision of the manuscript:** V.E. Zannella, A. Dal Pra, H. Muaddi, T.D. McKee, S. Stapleton, J. Sykes, M. Milosevic, B.G. Wouters, R.G. Bristow, M. Koritzinsky

**Administrative, technical, or material support (i.e., reporting or organizing data, constructing databases):** V.E. Zannella, A. Dal Pra, H. Muaddi, T.D. McKee, R.G. Bristow

**Study supervision:** B.G. Wouters, R.G. Bristow, M. Koritzinsky

#### Acknowledgments

The authors thank Stephen Chung and Kitty Ki for technical assistance.

#### Grant Support

This work was financially supported in part by the Ontario Ministry of Health and Long Term Care (OMOHLTC), The Princess Margaret Cancer Foundation (IDEAS to M. Koritzinsky), The Terry Fox Foundation/Research Institute (New Frontiers Research Program PPG09-020005 to B.G. Wouters, R.G. Bristow, M. Koritzinsky and New Investigator Award to M. Koritzinsky), the Ontario Institute for Cancer Research (B.G. Wouters, R.G. Bristow and SITARR), Government of Ontario (B.G. Wouters), Canadian Foundation for Innovation (SITARR), Canadian Cancer Society (Research Scientist award to R.G. Bristow), Canadian Urology Oncology Group (Research award to A. Dal Pra), University of Toronto (Paul Starita Fellowship to V.E. Zannella), Comprehensive Research Experience for Medical Students Program (award to H. Muaddi). The views expressed do not necessarily reflect those of the OMOHLTC.

The costs of publication of this article were defrayed in part by the payment of page charges. This article must therefore be hereby marked *advertisement* in accordance with 18 U.S.C. Section 1734 solely to indicate this fact.

Received June 28, 2013; revised September 4, 2013; accepted September 28, 2013; published OnlineFirst October 18, 2013.

#### References

- Nordsmark M, Bentzen SM, Rudat V, Brizel D, Lartigau E, Stadler P, et al. Prognostic value of tumor oxygenation in 397 head and neck tumors after primary radiation therapy. An international multi-center study. *Radiother Oncol* 2005;77:18–24.
- Milosevic M, Warde P, Menard C, Chung P, Toi A, Ishkanian A, et al. Tumor hypoxia predicts biochemical failure following radiotherapy for clinically localized prostate cancer. *Clin Cancer Res* 2012;18:2108–14.
- Wouters BG, Wepler SA, Koritzinsky M, Landuyt W, Nuyts S, Theys J, et al. Hypoxia as a target for combined modality treatments. *Eur J Cancer* 2002;38:240–57.
- Ljungkvist AS, Bussink J, Kaanders JH, van der Kogel AJ. Dynamics of tumor hypoxia measured with bioreductive hypoxic cell markers. *Radiat Res* 2007;167:127–45.
- Overgaard J. Hypoxic modification of radiotherapy in squamous cell carcinoma of the head and neck—a systematic review and meta-analysis. *Radiother Oncol* 2011;100:22–32.
- Janssens GO, Rademakers SE, Terhaard CH, Doornaert PA, Bijl HP, van den Ende P, et al. Accelerated radiotherapy with carbogen and nicotinamide for laryngeal cancer: results of a phase III randomized trial. *J Clin Oncol* 2012;30:1777–83.
- Overgaard J. Hypoxic radiosensitization: adored and ignored. *J Clin Oncol* 2007;25:4066–74.
- Seomb TW, Hsu R, Ong ET, Gross JF, Dewhirst MW. Analysis of the effects of oxygen supply and demand on hypoxic fraction in tumors. *Acta Oncol* 1995;34:313–6.
- Biaglow JE, Durand RE. The effects of nitrobenzene derivatives on oxygen utilization and radiation response of an *in vitro* tumor model. *Radiat Res* 1976;65:529–39.
- Durand RE, Biaglow JE. Radiosensitization of hypoxic cells of an *in vitro* tumor model by respiratory inhibitors. *Radiat Res* 1977;69:359–66.
- Durand RE, Biaglow JE, Greenstock CL. Effects of sensitizers on cell respiration. III. The effects of hypoxic cell radiosensitizers on oxidative

- metabolism and the radiation response of an in vitro tumour model. *Br J Cancer Suppl* 1978;3:150-3.
12. Biaglow JE, Durand RE. The enhanced radiation response of an in vitro tumour model by cyanide released from hydrolysed amygdalin. *Int J Radiat Biol Relat Stud Phys Chem Med* 1978;33:397-401.
  13. Lee I, Glickson JD, Dewhirst MW, Leeper DB, Burd R, Poptani H, et al. Effect of mild hyperglycemia +/- meta-iodo-benzylguanidine on the radiation response of R3230 Ac tumors. *Adv Exp Med Biol* 2003;530:177-86.
  14. Diepart C, Karroum O, Magat J, Feron O, Verrax J, Calderon PB, et al. Arsenic trioxide treatment decreases the oxygen consumption rate of tumor cells and radiosensitizes solid tumors. *Cancer Res* 2012;72:482-90.
  15. Viollet B, Guigas B, Sanz Garcia N, Leclerc J, Foretz M, Andreelli F. Cellular and molecular mechanisms of metformin: an overview. *Clin Sci* 2012;122:253-70.
  16. Owen MR, Doran E, Halestrap AP. Evidence that metformin exerts its anti-diabetic effects through inhibition of complex 1 of the mitochondrial respiratory chain. *Biochem J* 2000;348 Pt 3:607-14.
  17. Davidoff F. Effects of guanidine derivatives on mitochondrial function. I. Phenethylbiguanide inhibition of respiration in mitochondria from guinea pig and rat tissues. *J Clin Invest* 1968;47:2331-43.
  18. Kreso A, O'Brien CA. Colon cancer stem cells. *Curr Protoc Stem Cell Biol* 2008;7:3.1.-13.1.12.
  19. Locke JA, Zafarana G, Ishkian AS, Milosevic M, Thoms J, Have CL, et al. NKX3.1 haploinsufficiency is prognostic for prostate cancer relapse following surgery or image-guided radiotherapy. *Clin Cancer Res* 2012;18:308-16.
  20. Bergstrahl E, Kosanke J. Computerized matching of cases to controls using the greedy matching algorithm with a fixed number of controls per case (gmatch) [SAS macro]. Mayo Clinic Division of Biostatistics; 2003. Available from: <http://www.mayo.edu/research/departments-divisions/department-health-sciences-research/division-biomedical-statistics-informatics/software/locally-written-sas-macros>.
  21. Austin PC, Grootendorst P, Anderson GM. A comparison of the ability of different propensity score models to balance measured variables between treated and untreated subjects: a Monte Carlo study. *Stat Med* 2007;26:734-53.
  22. Sharma V, McNeill JH. To scale or not to scale: the principles of dose extrapolation. *Br J Pharmacol* 2009;157:907-21.
  23. Dowling RJ, Goodwin PJ, Stambolic V. Understanding the benefit of metformin use in cancer treatment. *BMC Med* 2011;9:33.
  24. Algire C, Amrein L, Bazile M, David S, Zakikhani M, Pollak M. Diet and tumor LKB1 expression interact to determine sensitivity to anti-neoplastic effects of metformin in vivo. *Oncogene* 2011;30:1174-82.
  25. Shackelford DB, Abt E, Gerken L, Vasquez DS, Seki A, Leblanc M, et al. LKB1 inactivation dictates therapeutic response of non-small cell lung cancer to the metabolism drug phenformin. *Cancer Cell* 2013;23:143-58.
  26. Storozhuk Y, Hopmans SN, Sanli T, Barron C, Tsiani E, Cutz JC, et al. Metformin inhibits growth and enhances radiation response of non-small cell lung cancer (NSCLC) through ATM and AMPK. *Br J Cancer* 2013;108:2021-32.
  27. Sanli T, Rashid A, Liu C, Harding S, Bristow RG, Cutz JC, et al. Ionizing radiation activates AMP-activated kinase (AMPK): a target for radiosensitization of human cancer cells. *Int J Radiat Oncol Biol Phys* 2010;78:221-9.
  28. Song CW, Lee H, Dings RP, Williams B, Powers J, Santos TD, et al. Metformin kills and radiosensitizes cancer cells and preferentially kills cancer stem cells. *Sci Rep* 2012;2:362.
  29. Liu J, Hou M, Yuan T, Yi G, Zhang S, Shao X, et al. Enhanced cytotoxic effect of low doses of metformin combined with ionizing radiation on hepatoma cells via ATP deprivation and inhibition of DNA repair. *Oncol Rep* 2012;28:1406-12.
  30. Skinner HD, Sandulache VC, Ow TJ, Meyn RE, Yordy JS, Beadle BM, et al. TP53 disruptive mutations lead to head and neck cancer treatment failure through inhibition of radiation-induced senescence. *Clin Cancer Res* 2012;18:290-300.
  31. Muaddi H, Chowdhury S, Vellanki R, Zamiara P, Koritzinsky M. Contributions of AMPK and p53 dependent signaling to radiation response in the presence of metformin. *Radiother Oncol* 2013. [Epub ahead of print].
  32. Wilcock C, Bailey CJ. Accumulation of metformin by tissues of the normal and diabetic mouse. *Xenobiotica* 1994;24:49-57.
  33. Carlson DJ, Keall PJ, Loo BW Jr, Chen ZJ, Brown JM. Hypofractionation results in reduced tumor cell kill compared to conventional fractionation for tumors with regions of hypoxia. *Int J Radiat Oncol Biol Phys* 2011;79:1188-95.
  34. Brown JM, Diehn M, Loo BW Jr. Stereotactic ablative radiotherapy should be combined with a hypoxic cell radiosensitizer. *Int J Radiat Oncol Biol Phys* 2010;78:323-7.
  35. Buyyounouski MK, Pickles T, Kestin LL, Allison R, Williams SG. Validating the interval to biochemical failure for the identification of potentially lethal prostate cancer. *J Clin Oncol* 2012;30:1857-63.
  36. Margel D, Urbach DR, Lipscombe LL, Bell CM, Kulkarni G, Austin PC, et al. Metformin use and all-cause and prostate cancer-specific mortality among men with diabetes. *J Clin Oncol* 2013;31:3069-75.
  37. Skinner HD, McCurdy MR, Echeverria AE, Lin SH, Welsh JW, O'Reilly MS, et al. Metformin use and improved response to therapy in esophageal adenocarcinoma. *Acta Oncol* 2013;52:1002-9.

# Clinical Cancer Research

## Reprogramming Metabolism with Metformin Improves Tumor Oxygenation and Radiotherapy Response

Vanessa E. Zannella, Alan Dal Pra, Hala Muaddi, et al.

*Clin Cancer Res* 2013;19:6741-6750. Published OnlineFirst October 18, 2013.

**Updated version** Access the most recent version of this article at:  
[doi:10.1158/1078-0432.CCR-13-1787](https://doi.org/10.1158/1078-0432.CCR-13-1787)

**Supplementary Material** Access the most recent supplemental material at:  
<http://clincancerres.aacrjournals.org/content/suppl/2013/10/21/1078-0432.CCR-13-1787.DC1>

**Cited articles** This article cites 34 articles, 9 of which you can access for free at:  
<http://clincancerres.aacrjournals.org/content/19/24/6741.full#ref-list-1>

**Citing articles** This article has been cited by 16 HighWire-hosted articles. Access the articles at:  
<http://clincancerres.aacrjournals.org/content/19/24/6741.full#related-urls>

**E-mail alerts** [Sign up to receive free email-alerts](#) related to this article or journal.

**Reprints and Subscriptions** To order reprints of this article or to subscribe to the journal, contact the AACR Publications Department at [pubs@aacr.org](mailto:pubs@aacr.org).

**Permissions** To request permission to re-use all or part of this article, use this link <http://clincancerres.aacrjournals.org/content/19/24/6741>. Click on "Request Permissions" which will take you to the Copyright Clearance Center's (CCC) Rightslink site.